The large wave corresponding to the catalyzed reduction of O_2 is well-separated from the surface wave for the reduction of adsorbed $Co^{III}TMPyP$. Although the O_2 reduction wave appears in the same vicinity as the *solution* formal potential of the $Co^{III/II}$ couple, the dissolved porphyrin contributes little or nothing to the catalysis because the catalytic current is not diminished when the electrode is transferred to a solution containing no dissolved $Co^{III}TMPyP$ (Figure 4B). Thus, adsorbed CoTMPyP, with a formal potential near 0.5 V catalyzes the reduction of O_2 at potentials near 0.23 V.

The greater visibility of the wave for the reduction of dissolved CoTMPyP in steady-state rotating disk current–potential curves (Figure 2B) than in cyclic voltammograms (Figure 1) is attributable, in part, to the relatively high background current that flows at edge-plane graphite electrodes when their potentials are scanned at the 100–200 mV s^{-1} rates that are typical of cyclic voltammetry.

The rate of oxidation of $Co^{II}TMPyP$ by O_2 was examined spectrophotometrically by mixing the two reactants and monitoring the spectra of the resulting solution in the region between 400 and 500 nm. In 0.1 M H_2SO_4 saturated with air, an electrolyte similar to that employed in some previous studies,[5,13,14] the spectrum observed matched that reported for $Co^{II}TMPyP$[3] for at least 60 s after mixing; even after 1 h the oxidation was less than 50% complete. Addition of a slight excess of Fe^{3+} produced an immediate conversion to the spectrum of $Co^{III}TMPyP$.[3] The oxidation of $Co^{II}TMPyP$ (5 μM) by O_2 in 0.5 M trifluoroacetic acid, the electrolyte employed in this study, proceeds somewhat more rapidly, but the half-life of $Co^{II}TMPyP$ is still over 5 min. Thus, $Co^{II}TMPyP$ and O_2 can coexist in solution for periods that are long compared to the time required for reactants to cross the diffusion layer in typical cyclic or rotating disk voltammetric experiments (0.1–1 s).

The large difference in the Co(III/II) formal potentials between adsorbed and unadsorbed CoTMPyP as measured with graphite electrodes indicates unusually favorable interactions between the cobalt center and the electrode surface when the cobalt is in the reduced state. It has been suggested in previous studies[10] that organic functional groups known to be present on the graphite surface may serve as ligands that stabilize Co(II) more than Co(III). Whatever the origin of the shift in formal potential, it is responsible for the separation between the potentials where the cobalt center exhibits its redox activity and the potentials where the porphyrin catalyzes the reduction of O_2. Because of the magnitude and direction of this separation, the mechanism of the catalysis is best regarded as "CE catalytic". That is, the O_2 substrate undergoes a chemical reaction (C) with the (reduced) catalyst that precedes its electrochemical reduction (E). Since the reduced catalyst and substrate can coexist in solution for periods that are long compared with the effective measurement times in electrochemical experiments, the "EC catalytic" mechanism (in which catalyst reduction triggers substrate reduction) that has been proposed for some porphyrin-catalyzed electroreductions of O_2[5,13,14] is clearly inapplicable to the present case.[11] The fact that the catalyzed reduction of O_2 proceeds not far from the formal potential of the $Co^{III/II}$ couple for the unadsorbed porphyrin is coincidental and does *not* imply that outer-sphere electron transfer between O_2 and the reduced catalyst is the rate-limiting step.

The literature now contains reports on the catalysis of the electroreduction of O_2 by a variety of cobalt porphyrins that includes both water-soluble and water-insoluble examples. Table I is a summary of the reported formal redox potentials of the cobalt porphyrins and of the potentials where they exhibit catalytic activity toward the reduction of O_2. The pattern that emerges from the potentials listed in Table I is of catalysts that exhibit redox activity in the adsorbed state at potentials more positive than those where they catalyze O_2 reduction and those where the

dissolved porphyrin is electroactive. The redox activity of the dissolved cobalt porphyrin catalysts appears at potentials on both sides of those where O_2 reduction proceeds as would be expected if the dominant catalytic pathway involved the (inevitably present) adsorbed catalyst.

Contribution from the Institut für Physikalische und Theoretische Chemie, Universität Tübingen, 7400 Tübingen, West Germany, and Department of Chemistry, University of Idaho, Moscow, Idaho 83843

Gas-Phase Structure of Perfluoronitrosocyclobutane

Helen M. Marsden,[1b] Heinz Oberhammer,*[1a] and Jean'ne M. Shreeve[1b]

While a rather large number of acyclic nitrosofluoroalkanes have been synthesized, only a few nitrosofluoro aromatic compounds and only two fluoronitrosocycloalkanes are known.[2] In the present case, perfluoronitrosocyclobutane, it is of interest to examine the effect of the substituent on the geometry of the ring relative to perfluorocyclobutane and to compare the orientation of the NO group and structural data of the cyclic compound with that of acyclic perfluoronitrosoalkanes.

Perfluoronitrosocyclobutane was prepared from nitrosyl chloride and perfluorocyclobutane in the presence of anhydrous potassium fluoride and acetonitrile.[2] The sample was purified on a Hewlett-Packard 5710 A gas chromatograph equipped with Valco gas sample injection valves. The separation was done on a 11 ft × $^1/_4$ in. column containing 25% w/w Kel-F oil No. 3 on Chromosorb P maintained at room temperature. The injection and detector temperature was 100 °C. The sample was transferred from Idaho to Germany under liquid nitrogen.

The electron diffraction intensities were recorded on 13 × 18 cm Kodak Electron Image plates with a Balzers KD-G2 gas diffractograph[3] at two camera distances (25 and 50 cm). The accelerating voltage was about 60 kV. The sample was kept at about −50 °C during the experiment, and the inlet system and nozzle (0.25 mm diameter) were at room temperature. The background pressure in the diffraction chamber never exceeded 2×10^{-5} torr. Exposure times were 5–10 and 25–35 s for the long and short camera distances respectively. The electron wavelength was determined from ZnO diffraction patterns. Two plates for each camera distance were analyzed by the usual procedure[4] and the averaged molecular intensities for the *s* ranges 1.4–17 and 8–35 Å^{-1} in steps of $\Delta s = 0.2$ Å^{-1} are presented in Figure 1.

Six possible conformations have to be considered for perfluoronitrosocyclobutane, depending on the position (axial or equatorial) and orientation (endo, exo, or gauche) of the nitroso group. A preliminary analysis of the radial distribution function (Figure 2) indicates that both exo conformers (ax-exo and eq–exo) are compatible with the experiment. A clear distinction between axial or equatorial position of the NO group is not possible. In the least-squares analysis a diagonal weight matrix was applied to the molecular intensities and scattering amplitudes and phases of ref 5 were used. The following constraints were introduced: (1) C–C and C–F bond lengths were made equal; (2) the N–O

(1) (a) Universität Tübingen. (b) University of Idaho.
(2) Marsden, H. M.; Shreeve, J. M. *Inorg. Chem.* **1984**, *23*, 3654.
(3) Oberhammer, H. "Molecular Structures by Diffraction Methods"; The Chemical Society: London, 1976; Vol. 4, pp 24–44.
(4) Oberhammer, H.; Gombler, W.; Willner, H. *J. Mol. Struct.* **1980**, *70*, 273.
(5) Haase, J. *Z. Naturforsch., A* **1968**, *23*, 1000.

(13) Bettelheim, A.; Chan, R. J. H.; Kuwana, T. *J. Electroanal. Chem. Interfacial Electrochem.* **1979**, *99*, 391.
(14) Ozer, D.; Parash, R.; Broitman, F.; Mor, U.; Bettelheim, A. *J. Chem. Soc., Faraday Trans. 1* **1984**, *80*, 1139.
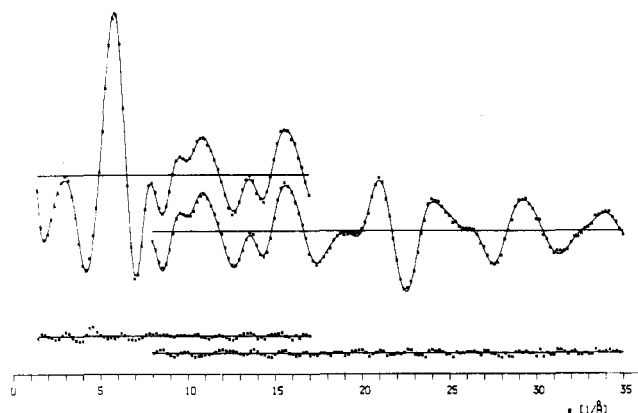
Figure 1. Experimental (···) and calculated (—) molecular intensities and differences for the eq-exo conformer.
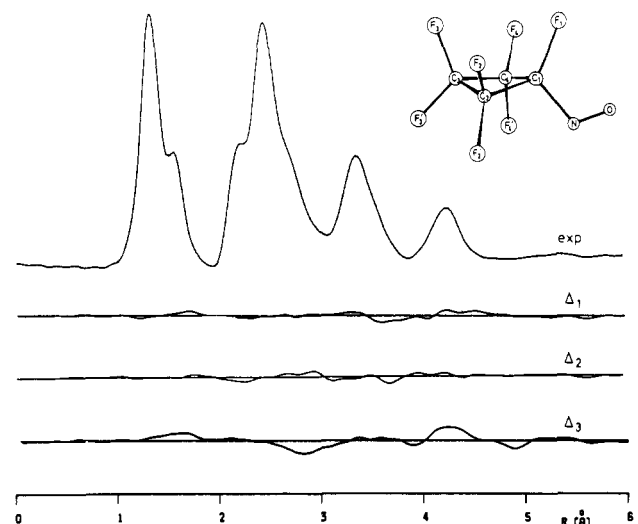

Figure 2. Experimental radial distribution function and difference curves for eq-exo (Δ_1), ax-exo (Δ_2), and ax-gauche conformations (Δ_3). The molecular model with atom numbering corresponds to the eq-exo conformer.

Table I. Results of Least-Squares Refinement for the Eq-exo Conformer[g]

(a) Geometric Parameters (r_g Values (Å) for Distances, r_a Values (deg) for Angles)

(C–C)$_{av}$ (p_1)	1.573 (5)	FCF (p_5)	109.1 (4)
(C–F)$_{av}$ (p_2)	1.331 (3)	F$_3$CN (p_6)	109.7 (21)
C–N (p_3)	1.521 (15)	ρ^b (p_7)	0.7 (11)
N=O	1.20^a	θ^c (p_8)	23.0 (18)
C$_2$C$_1$C$_4$ (p_4)	91.4 (6)	CNO (p_9)	111.9 (22)
C$_1$C$_2$C$_3$^{d}	86.3 (6)		

(b) Interatomic Distances (Å) and Vibrational Amplitudes

atom pair	dist	m^e	amplitude	atom pair	dist	m	amplitude
N=O	1.20	1	0.040^a	F$_1$···F$_3'$	3.21	1	
C–F	1.33	7	0.047 (2)	C$_1$···F$_3$	3.25	1	
C–N	1.52	1	} 0.050 (5)	C$_2$···F$_4$	3.34	2	} 0.100^a
C–C	1.57	4		F$_2$···F$_3'$	3.34	2	
C$_1$···C$_3$	2.15	1		F$_2'$···F$_4'$	3.35	1	
C$_2$···C$_4$	2.25	1		N···C$_3$	3.43	1	
F···F''	2.17	3	} 0.051 (6)	C$_2$···O	3.48	2	
C$_1$···O	2.26	1		N···F$_2$	3.49	2	} 0.110 (10)
N···F$_1$	2.33	1		F$_1$···F$_2'$	3.52	2	
O···F$_1$	2.42	1		F$_2'$···F$_3$	3.52	2	
C$_2$···F$_1$	2.43	2		F$_2'$···O	3.79	2	
C$_2$···F$_3$	2.44	4	} 0.071 (4)	O···F$_2$	4.07	2	
C$_1$···F$_2$	2.45	8		F$_2$···F$_4'$	4.18	1	
N···C$_2$	2.60	1		F$_1$···F$_3'$	4.22	1	} 0.135 (55)
F$_1$···F$_2$	2.68	2		N···F$_3$	4.24	1	
F$_2$···F$_3'$	2.69	2	} 0.110 (6)	F$_2'$···F$_4'$	4.32	2	
F$_3$···F$_3'$	2.70	2		C$_3$···O	4.38	1	} 0.150^a
N···F$_2$	2.79	2		N···F$_3$	4.42	1	
C$_3$···F$_1$	2.94	1		O···F$_3$	5.19	1	} 0.200^a
C$_1$···F$_3'$	2.95	1	} 0.080 (19)	O···F$_3'$	5.34	1	
C$_2$···F$_4$	3.05	2					

(c) Agreement Factors[f]

$$R_{50} = 0.052 \qquad R_{25} = 0.091$$

^{a} Not refined. ^{b} Rock angle of F$_1$CN such that F$_1$···F$_3$ come closer together. ^{c} Puckering angle between the planes C$_2$C$_1$C$_4$ and C$_2$C$_3$C$_4$. ^{d} Dependent angle. ^{e} Multiplicity of distance. $^f R = (\Sigma w_i \Delta_i^2 / \Sigma w_i M_i (\text{exptl})^2)^{1/2}$, $\Delta_i = M_i(\text{exptl}) - M_i(\text{calcd})$, and w_i is the weighing function. ^{g} Error limits are 3σ values and include a possible scale error of 0.1% for bond lengths.

distance was fixed at 1.20 Å (N–O = 1.197 (5)[6] or 1.198 (4) Å[7] in CF$_3$NO); (3) C_{2v} symmetry was given to the CF$_2$ groups (i.e no rock, twist, or wag angle). The vibrational amplitudes were grouped according to their distances, and this grouping was different for each conformation considered (see Table I for eq-exo conformer). Refinements for endo and gauche orientations of the NO group result in poor agreement between experimental and calculated radial distribution functions in the distance range $r > 2.5$ Å, for both axial and equatorial positions. The agreement factors (for definition see footnote to Table I) for the 50-cm data increase by 70, 160, 40, and 90%, respectively, for the eq-endo, ax-endo, eq-gauche, and ax-gauche conformers over the corresponding exo forms. The increase of the agreement factors for the 25-cm data is smaller. The difference curve for the ax-gauche conformer (Δ_3) is shown in Figure 2. In addition to the increased agreement factors, endo and gauche orientations of the nitroso group result in unreasonably small or large values for some nonbonded vibrational amplitudes and can be excluded. Both exo conformers, eq-exo and ax-exo, however, fit the experimental intensities almost equally well (see difference curves Δ_1 and Δ_2 in Figure 2). The geometric parameters for both conformers are equal within their experimental uncertainties, except for the CNO angle. This angle is 106.3 (18)° for the axial and 111.9 (21)° for the equatorial conformer. The former value is rather small when compared to CNO angles in other compounds (e.g. 112.6 (10)° in CH$_3$NO[8] and 113.2 (13) or 112.4 (3)° in CF$_3$NO[6,7]).

On the basis of these CNO bond angles, the equatorial conformer should be slightly favored, but a mixture of both conformers is as likely. The electron diffraction data do not allow any conclusion concerning the ratio of both conformers. The final results for the eq-exo conformer are summarized in Table I. Error limits are 3σ values and include a possible scale error of 0.1% for the bond lengths. The following correlations had values larger than |0.6|: $p_4/p_6 = -0.89$, $p_4/p_7 = 0.72$, $p_4/p_8 = 0.63$, $p_5/p_6 = 0.61$, $p_6/p_7 = -0.86$, $p_6/p_8 = -0.81$, $p_7/p_8 = 0.84$, and $p_7/p_9 = -0.73$.

The geometry of the fluorinated four-membered ring in perfluoronitrosocyclobutane agrees with that of two earlier studies of perfluorocyclobutane: C–C = 1.572 (5) Å vs. 1.566 (8)[9] and 1.560 (9) Å,[10] C–F = 1.330 (3) Å vs. 1.324 (5)[9] and 1.333 (2) Å,[10] θ = 23.0 (18)° vs. 17.4 (3)°[9] and 24.0 (30)°,[10] FCF = 109.1 (4)° vs. 109.9 (3)°[9] and 109.0 (10)°.[10] Comparison with the parent compound C$_4$H$_8$ demonstrates that fluorination of the ring results in lengthening of the C–C bonds and flattening of the ring (C–C = 1.551 (3) Å and θ = 28.7 (10)° in C$_4$H$_8$[11]). The C–N bond (1.521 (15) Å) is longer than expected for a N(sp^2)–C(sp^3) bond (e.g. 1.460 (6) Å in CF$_3$N=NCF$_3$[12] or 1.400 (10) Å in CF$_3$NCO[13]). The long C–N bond, however, is in agreement with the values determined for CF$_3$NO (1.546 (8)[6] and 1.512 (16) Å[7]).

(6) Bauer, S. H.; Andreassen, A. L. *J. Phys. Chem.* **1972**, *76*, 3099.
(7) Turner, P. H.; Cox, A. P. *Chem. Phys. Lett.* **1976**, *39*, 585.

(8) Coffey, D.; Britt, C. O.; Boggs, J. E. *J. Chem. Phys.* **1968**, *49*, 591.
(9) Chiang, J. F.; Porter, R. F.; Bauer, S. H. *J. Mol. Struct.* **1971**, *7*, 89.
(10) Alekseev, N. V.; Barzdain, P. P. *J. Struct. Chem. (Eng. Transl.)* **1974**, *15*, 171.
(11) Kuchitsu, K. Seventh Austin Symposium on Gas Phase Molecular Structure, Austin, TX, 1978.
(12) Bürger, H.; Pawelke, G.; Oberhammer, H. *J. Mol. Struct.* **1982**, *84*, 49.
(13) Steger, B.; Oberhammer, H., unpublished observations.

The exo orientation of the NO group in C_4F_7NO, i.e. eclipsed position with respect to F_1, corresponds to the eclipsed conformation observed for CF_3NO. No gas-phase structural data are known for a nitroso or isoelectronic carboxaldehyde group bonded to cyclobutane, which would allow comparison of the position of such groups relative to the ring. In nitrosocyclopropane the preference for the exo orientation of the NO group has been determined by microwave spectroscopy and no transitions corresponding to any other orientation were observed.[14] For cyclopropanecarboxaldehyde both conformers, exo and endo, are nearly equally favored[15] and this result is in agreement with theoretical considerations.[16]

The nitroso group causes considerable angle distortion of the cyclobutane ring ($C_2C_1C_4 = 91.4$ (6)° vs. $C_1C_2C_3 = 86.3$ (6)°), resulting in a shorter $C_1 \cdots C_3$ distance (2.15 Å) than $C_2 \cdots C_4$ distance (2.25 Å).

(14) Corkill, M. J.; Cox, A. P.; Norris, J. A. *J. Chem. Soc., Chem. Commun.* **1978,** 388.
(15) Bartell, L. S.; Guillory, J. P. *J. Chem. Phys.* **1965,** *43,* 647.
(16) Hoffmann, R.; Davidson, R. B. *J. Am. Chem. Soc.* **1971,** *93,* 5699.

Contribution from the Department of Chemistry
and Institute of Materials Science,
The University of Connecticut, Storrs, Connecticut 06268

Theoretical Investigation of the Molecular Structure of Manganese Dichloride

Magdolna Hargittai*[1] and Angelo R. Rossi*

The present theoretical investigation is an extension of previous experimental electron diffraction studies of the molecular structure of first-row transition-metal dihalides: $MnCl_2$,[2] $MnBr_2$,[3] $FeCl_2$,[4] $FeBr_2$,[4] $CoCl_2$,[5] $CoBr_2$,[6] and $NiBr_2$.[7] These studies have pointed to a linear configuration for these molecules while exhibiting large-amplitude, low-frequency bending vibrations. Current electron diffraction analyses of the molecular structure of vanadium dichloride[8] and chromium dichloride,[8] however, indicate that these molecules may have a highly bent structure with bond angles in the vicinity of 110°. These analyses are in progress and are indeed complicated by the presence of different amounts of dimeric species. Such mixtures have been successfully analyzed for manganese dibromide[3] and iron dibromide[4] as well as for cobalt dibromide.[6] The emerging bent monomeric structures for VCl_2 and $CrCl_2$, however, prompted us to initiate a theoretical investigation on the geometry and electronic structure of the ground-state dichloride monomeric species. As a benchmark for further

calculations on other transition-metal dichlorides, the manganese dichloride molecule was chosen. The choice of $MnCl_2$ was motivated both by the relative ease of computation for the d^5 configuration and by the good experimental electron diffraction data available for this molecule.[2] Our calculations were essentially completed when a recent matrix-isolation infrared spectroscopic study[9] came to our attention, reporting a bent structure for the dichlorides of iron, cobalt, and nickel, with a bond angle of about 160°. The electron diffraction data on all these molecules have been interpreted with a linear equilibrium configuration; $FeCl_2$ and $CoCl_2$ have been studied in our Budapest laboratory,[4,5] and the structure of $NiCl_2$ has been determined in Professor Hedberg's laboratory.[10] The apparent controversy has already been commented upon.[11] A reanalysis of the electron scattering data of iron dichloride and additional spectroscopic calculations[11] reinforce the linear structure for this molecule. Calculations on magnanese dichloride are instructive also in this respect since the electron diffraction analyses led to analogous results for the whole series of $MnCl_2$, $FeCl_2$, $CoCl_2$, and $NiCl_2$ molecules.

The low-frequency, large-amplitude bending vibrations and the high-temperature experimental conditions make the electron diffraction analysis of a molecule like manganese dichloride less straightforward than those of more rigid molecules. For this reason the experimental results[2] will be briefly summarized. The nozzle temperature of the manganese dichloride experiment was approximately 800 °C. The thermally averaged internuclear distances[12] were determined to be $r_g(Mn-Cl) = 2.205 \pm 0.005$ Å and $r_g(Cl \cdots Cl) = 4.324 \pm 0.015$ Å. If the equilibrium confirguration is assumed to be linear, the $2r_g(Mn-Cl) - r_g(Cl \cdots Cl)$ difference is the linear shrinkage, $\delta_g = 0.086$ Å. This shrinkage is the consequence of large-amplitude bending vibrations, and under this assumption it was used to estimate the bending vibrational frequency, $\nu_2 = 93 \pm 8$ cm^{-1}. This estimated frequency compared well with the value 83 cm^{-1} reached from a matrix-isolation infrared spectroscopic investigation.[13] This rather good agreement, in fact, supported the assumption for the linear equilibrium configuration. Originally this assumption was based on the lack of the symmetric stretching frequency in the infrared spectrum[13] and the absence of a permanent electric dipole moment as concluded from the molecular beam deflection experiments.[14]

Although all experimental evidence is consistent with a linear equilibrium geometry, the experimental data refer directly to an average structure resulting from averaging over all intramolecular motion. On the other hand, the theoretical calculations refer directly to the equilibrium configurations. As the manganese dichloride study was considered to be a bench mark one for further calculations on other transition-metal dihalides, it was also decided to examine the applicability of various levels of basis set sophistication to determine a reasonable level of theory for use in future work.

Computational Details

All ab initio calculations were carried out with the GAMESS series of programs.[15] The structural parameters that were varied in the calculations are the Mn-Cl bond distance and the Cl-Mn-Cl bond angle. Restricted open-shell calculations for the open-shell sextet states were carried out by using Davidson's method.[16] The open shell calculations were performed on the $...1\delta_g^2 3\pi_g^2 g\sigma_g^1$ configuration for linear $D_{\infty h}$ geometry and $...3a_2^1 10b_2^1 13a_1^1 5b_1^1 14a_1^1$ configuration for bent C_{2v} geometries.

Several different basis sets were employed for the present calculations on $MnCl_2$. Basis I consists of the STO-3G basis of Hehre et al.,[17] which

(1) Visiting Scientist at The University of Connecticut (1983–1985), on leave from the Hungarian Academy of Sciences, Budapest H-1431, Hungary.
(2) Hargittai, I.; Tremmel, J.; Schultz, Gy. *J. Mol. Struct.* **1975,** *26,* 116.
(3) Hargittai, M.; Hargittai, I.; Tremmel, J. *Chem. Phys. Lett.* **1981,** *83,* 207.
(4) Vajda, E.; Tremmel, J.; Hargittai, I. *J. Mol. Struct.* **1978,** *44,* 101.
(5) Tremmel, J.; Ivanov, A. A.; Schultz, Gy.; Hargittai, I.; Cyvin, S. J.; Ericksson, A. *Chem. Phys. Lett.* **1973,** *23,* 533.
(6) Hargittai, M.; Dorofeeva, O. V.; Tremmel, J. *Inorg. Chem.* **1985,** *24,* 245.
(7) Molnar, Zs.; Schultz, Gy.; Tremmel, J.; Hargittai, I. *Acta Chim. Acad. Sci. Hung.* **1975,** *86,* 223.
(8) Dorofeeva, O. V.; Hargittai, M.; Tremmel, J. Tenth Austin Symposium on Molecular Structure *1984.* Austin, TX, 1984; Paper A13, p 93.

(9) Green, D. W.; McDermott, D. P.; Bergman, A. *J. Mol. Spectrosc.* **1983,** *98,* 111.
(10) Eddy, L. Ph.D. Dissertation, Oregon State University, Corvallis, OR, 1973.
(11) Hargittai, M.; Hargittai, I. *J. Mol. Spectrosc.* **1984,** *108,* 159.
(12) E.g.; Kuchitsu, K. In "Diffraction Studies on Non-Crystalline Substances"; Hargittai, I., Orville-Thomas, W. J., Eds.; Akademiai Kiado: Budapest, Elsevier: Amsterdam, New York, 1981.
(13) Thompson, K. R.; Carlson, K. D. *J. Chem. Phys.* **1968,** *49,* 4379.
(14) Büchler, A.; Stauffer, J L.; Klemperer, W. *J. Am. Chem. Soc.* **1964,** *86,* 4544.
(15) Dupuis, M.; Spangler, D.; Wendoloski, J. J. QCPE **1981,** *1,* 91.
(16) Davidson, E. R. *Chem. Phys. Lett.* **1973,** *21,* 565.